

TBA: Faster Large Language Model Training Using SSD-Based Activation Offloading

Kun Wu*

Jeongmin Brian Park*
kunwu2@illinois.edu
jpark346@illinois.edu
University of Illinois at
Urbana-Champaign
USA

Vikram Sharma Malthody

vmailthody@nvidia.com
Nvidia
USA

Xiaofan Zhang*

xiaofanz@google.com
Google
USA

Sitao Huang

sitaoh@uci.edu
University of California, Irvine
USA

Mert Hidayetoğlu

merth@stanford.edu
Stanford University
USA

Steven Sam Lumetta

lumetta@illinois.edu
University of Illinois at
Urbana-Champaign
USA

Wen-mei Hwu

whwu@nvidia.com
Nvidia /
University of Illinois at
Urbana-Champaign
USA

Abstract

The growth rate of the GPU memory capacity has not been able to keep up with that of the size of large language models (LLMs), hindering the model training process. In particular, activations—the intermediate tensors produced during forward propagation and reused in backward propagation—dominate the GPU memory use. To address this challenge, we propose TBA to efficiently offload activations to high-capacity NVMe SSDs. This approach reduces GPU memory usage without impacting performance by adaptively overlapping data transfers with computation. TBA is compatible with popular deep learning frameworks like PyTorch, Megatron, and DeepSpeed, and it employs techniques such as tensor deduplication, forwarding, and adaptive offloading to further enhance efficiency. We conduct extensive experiments on popular LLMs like GPT, BERT, and T5. Results demonstrate that TBA effectively reduces 47% of the activation peak memory usage. At the same time, TBA perfectly overlaps the I/O with the computation and incurs negligible performance overhead. We introduce the recompute-offload-keep (ROK) curve to compare the TBA offloading with two other tensor placement strategies, keeping activations in GPU memory and layerwise full recomputation. We find that TBA achieves better memory savings than layerwise full recomputation while retaining the performance of keeping the activations in memory.

1 Introduction

Large language models (LLMs) now drive a wide range of applications, including chatbots [58], search [47], content generation [49], reasoning [37], etc. These models, when sufficiently large in size, demonstrate emergent abilities [88] and thus the capability of handling complicated tasks. Such a phenomenon drives model designers to continue to scale up the size of LLMs, carrying more parameters. The already formidably high training costs continue to grow: training GPT-4, for example, cost US\$100 million, a 21× increase over training GPT-3 [13].

GPU memory capacity has become a bottleneck for the continued growth of LLMs. As Figure 1 shows, the increase of GPU memory capacity is around 60% slower than the LLM size scaling speed and the GPU FP16 throughput improvement. About 80% of the GPU memory used to train recent LLMs consists of activations [35, 41], the intermediate tensors produced by forward propagation and reused in backward propagation. Furthermore, the memory needed for activations is growing more rapidly than any other memory use, making GPU memory a more serious constraint for future LLM training (see Section 2.2 for details).

Common mitigations are to reduce batch size or through gradient accumulation. With gradient accumulation, a batch is divided into micro-batches that are processed separately between gradient updates. Although gradient accumulation has been adopted by many LLMs [28, 77, 90], the GPU computation stack is not designed for small inputs, and both

*Equal contribution.

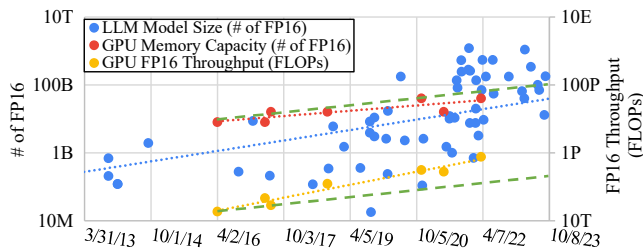


Figure 1. The growth of FP16 throughput (right vertical axis) of GPUs for deep learning training is aligned with the model size of LLMs (left vertical axis), but GPU memory capacity (left vertical axis) falls behind [84]. Horizontal axis shows release date. Points represent both Nvidia 100-level GPUs since K100 and Google TPUs. The auxiliary parallel green dash line grows at 50% the growth rate of FP16 throughput (yellow dash line), and the former grows faster than the memory capacity growth rate (red dash line).

mitigations lead to device under-utilization [4, 8] and sub-optimal math library performance [2]. Intuitively, a smaller batch size might reduce total training computation through faster convergence. However, LLM trainers have identified a critical batch size to each model, below which convergence speed increases negligibly or even decreases [31, 45]. Notably, critical batch size grows during training, as training loss is reduced.

Another common approach to reducing GPU memory use is activation checkpointing. With this strategy, only some of the activations are kept in GPU memory, while others are flushed and then recomputed during backward propagation. For a model with L layers, activation checkpointing can reduce memory requirements from $O(L)$ to $O(\sqrt{L})$ [9]. However, as we show in Section 2.2, even this reduction is insufficient to eliminate the bottleneck posed by the GPU memory limits for future LLMs.

This work proposes TBA, a software framework that offloads activations to Non-Volatile Memory Express (NVMe) SSDs and reloads activations just before they are needed in backward propagation. TBA is able to overlap activation transfers fully with computation, thereby reducing activation memory usage without incurring significant performance overhead. SSDs are a more attractive target than main (CPU) memory for several reasons. First, as shown in Figure 2, clusters and cloud instances [21, 48, 51] are typically limited in host memory capacity, while SSDs offer much higher capacity. The limited host memory capacity is also consumed by input data, checkpointing buffers and other training management buffers, which further reduces the amount of memory available for activation offloading. Second, host memory bandwidth is shared across training management tasks and offloaded computation [30, 69, 82] running on the host CPU and can be quite limited and even unpredictable [5] for saving and restoring activations. In contrast, the SSD bandwidth



Figure 2. Current clusters and cloud instances usually have limited main memory [21, 48, 51].

can be dedicated to the activation offloading during training. Third, SSDs are more elastic, both by adding more SSDs and even PCIe switches if necessary—as well as through use of optional remote high-throughput storage [22, 43]. Such elasticity allows the data centers to keep up with the fast growing size of activations. In contrast, the memory capacity of GPU cloud instances and cluster nodes is much more difficult to extend.

This work makes the following main contributions.

1. To address the GPU memory capacity issue and the resulting GPU under-utilization during LLM model training, we design and implement the TBA framework to offload activations in LLM training to NVMe SSDs. We demonstrate the viability of TBA on large-scale systems by modeling the performance, estimated SSD lifespan and the required per-GPU PCIe bandwidth.
2. With all code in Python except for a tiny CUDA memory allocation API hooking library, TBA works with the latest PyTorch, and distributed frameworks including Megatron [77] and DeepSpeed [68]. We developed and tested TBA with Megatron-DeepSpeed [46] on a two-GPU node with $7\times$ Intel Optane SSDs.
3. TBA incurs almost no performance overhead because it overlaps the data transfer fully with computation. To achieve this, we introduce several optimization techniques, including tensor deduplication, tensor forwarding, and adaptive offloading algorithm.
4. Evaluation shows TBA achieves almost the same training time per step as the original system without TBA while reducing the activations peak memory use by up to 47%. We introduce the recompute-offload-keep (ROK) curve to compare the TBA offloading with two other tensor placement strategies, keeping activations in memory and layerwise full recomputation. TBA has the same performance as keeping activations in memory and lower memory peak compared with activation checkpointing.

Artifacts will be released with the publication of this paper.

2 Background

2.1 Transformer-Based LLM

Most LLM architectures, including GPT [64], are transformer-based [86]. As Figure 3(a) shows, the GPT model consists mainly of multiple transformer layers. Before transformer layers, GPT takes in the tokenized text and maps the tokens into dense vectors with positional information. The task determines the last part of the model architecture. For instance,

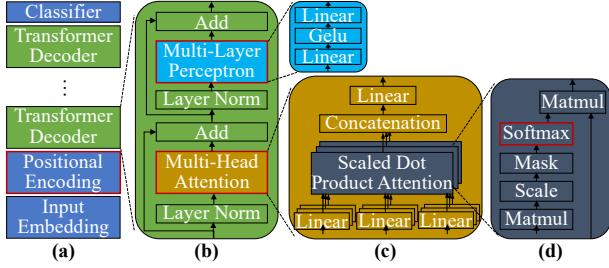


Figure 3. Hierarchical breakdown of the GPT model. In training, dropout is applied to the output of each layer with red borders.

a classifier could be added for text classification tasks. Figure 3(b) shows that each transformer layer is primarily made up of an attention block and a multi-layer perceptron (MLP) block. Attention blocks (Figure 3(c)) compute a weight, called attention, for each token pair, and produce dense vectors for each token via weighted summation. The MLP blocks transform the vector of each token into a new vector.

GPT is a decoder-only model because it only involves transformer decoder layers. A transformer encoder layer has the same structure as the transformer decoder layer except that the latter imposes causality on the attention mask in Figure 3(d): the causal mask ensures that the new vectors produced by the attention block for each token depend only on vectors of tokens, not after this token. By this categorization, transformer models are classified as (1) encoder-only, e.g., BERT [15], (2) decoder-only, e.g., GPT, Llama [85], and (3) encoder-decoder, e.g., T5 [65]. In encoder-decoder models, the transformer decoder layers take in both outputs from the encoders and another text and apply two attention blocks—the self-attention block is applied to the new text, and the cross-attention block is applied among the tokens in the sequence from the encoder and tokens in the new text.

Parallelizing LLM training involves partitioning and/or replicating the model and the data into different GPUs [91]. Pipeline parallelism, data parallelism, and model parallelism are the three levels of parallelism available to all LLM models and widely adopted in frameworks, e.g., Megatron, DeepSpeed, and PyTorch 2.0 [3, 68, 77]. Pipeline parallelism partitions the model into several chunks of layers and places them on different GPUs. In a step, when the GPUs finish their layers, the output is passed to the GPUs owning next layers. Data parallelism replicates the models in different groups of GPUs and assigns separate micro-batches to each group. At the end of a step, the gradients in each group are aggregated to update all the model replicas. Model parallelism shards a weight tensor and puts shards onto different GPUs. Each GPU performs a portion of the computation using its shard for the corresponding operator. Given the system scale and interconnect, all or a few among the three levels may be used. Zero Redundancy Optimizer (ZeRO) [66]

further reduce memory use with data parallelism by sharding the optimizer states, and/or optionally the gradients and parameters and store the shards across these GPUs.

2.2 GPU Memory Capacity and Model Throughput

As Figure 11 of Section 4 will show, the GPU memory capacity is limiting the model throughput. By offloading the activations to SSDs, TBA can alleviate this limitation and improve the per-GPU model throughput. An important question is if the GPU memory capacity will continue to be the limiting factor of per-GPU model throughput according to the trend of LLM scaling. This section shows that the historical trend will make GPU memory capacity an even more important limiting factor of the per-GPU model throughput.

Neural scaling laws [29, 31, 45] guide LLM scaling as computing power increases. We follow these laws in our reasoning. The whole-system GPU compute throughput $C \propto ND_{batch}$, where N is the number of parameters and D_{batch} is the number of tokens in a batch [6]. The Chinchilla scaling law [29] concludes that the optimal model design follows $N \propto C^{0.5}$, which implies $D_{batch} \propto C^{0.5}$ to saturate the GPU throughput. Whole-system GPU memory use consists of two parts: activations, which require $S_{activations} \propto \frac{N}{h}D_{batch}$, where h is the hidden dimension in the layers and is a slow growing function of N , e.g., $h \propto N^{1/3}$, and all other memory use, $S_{others} \propto N$, including parameters, gradients, and optimizer states. Comparing the factors, we can deduce that (1) $S_{activations}$ grows faster than S_{others} , and (2) whole-system memory use, which is dominated by the activations, grows slightly slower than the compute throughput C (approximated $C^{5/6}$). However, Figure 1 shows that the GPU memory capacity historically grows (red dash line) slower than even the the square root of the compute throughput (green dash line). Therefore, **GPU memory capacity will become increasingly inadequate for saturating the compute throughput, and memory for activations will continue to dominate the GPU memory usage.**

What about activation checkpointing? Revisiting the prior equation, $S_{activations} \propto \frac{N}{h}D_{batch} \propto LhD_{batch}$ where L is the number of layers. Activation checkpointing makes the new activations memory use $S'_{activations} \propto \sqrt{L}hD_{batch}$. Since L and h grow when N increases and $D_{batch} \propto C^{0.5}$, $S'_{activations}$ still grows faster than S_{others} .

2.3 SSD Endurance

Trends in price, latency, and bandwidth have led to the widespread adoption and integration of SSDs into cloud instances and clusters [21, 48, 51]. The random write latency of flash has been reduced to tens of microseconds [71], and NVMe SSD data rates are now a few GB/s.

	Kioxia FL6	Solidigm D7-P5620	Solidigm D7-P5810
3D NAND technology	96L SLC	144L TLC	144L SLC
Endurance rating (DWPD)	60	3	65 (sequential) 50 (random)
Max capacity	3.2 TB	12.8 TB	1.6 TB
Max endurance	342 PBW	65.4 PBW	146 PBW
Price per PBW	US\$13.9	US\$43.8	US\$11.1

Table 1. A sample of SSD models in mass production with high endurance in PB writes (PBW) [17, 34, 53, 73, 80, 81].

SSD endurance remains a concern: how long will SSDs last in a write-intensive scenario such as activation offloading? SSD endurance is determined by the type and numbers of cells, write amplification factor (WAF), and over-provisioning. SSD cells can be purposed to store one bit, i.e., single-level cells (SLCs), or multiple levels, e.g., triple-level cells (TLCs). Generally, the more bits a cell stores, the shorter its lifetime in program-erase (PE) cycles. WAF is the ratio of media write amount to host write amount—SSD writes pages at a time but erases blocks of pages, a coarser granularity. Erasing a partially empty block requires that remaining valid pages be relocated, causing write amplification. In turn, vendors adopt over-provisioning to reserve some blocks for wear leveling, evening out the writes across blocks.

Table 1 samples current SSD models. The D7-P5620 represents a mainstream data center model with 144-layer (L) TLC cells and a rating of 3 disk writes per day (DWPD). The FL6 and D7-P5810 SSDs are designed for write-intensive scenarios and have much higher endurance. Notably, SSD endurance rating uses the JESD testing method [27] which performs random writes after tough preconditioning. In our scenario, the writes are large, sequential writes as each tensor being offloaded is easily hundreds of MBs in size. Such writes are more endurance-friendly compared with the writes used to determine the JESD rating. For example, 3-DWPD SSDs generally allow about $2.5\times$ as many sequential writes than expected from the JESD rating [38, 63, 78]. Vendor guidelines [25, 72, 79] and empirical data [44] corroborate this difference. Section 3.4 conducts modeling to demonstrate why mainstream data center SSDs similar to D7-P5620 are viable options to support deployment of TBA in a large-scale LLM training system.

2.4 SSD Offloading Systems for LLM

GPUDirect Storage (GDS) enables a direct data path between GPU and local or remote NVMe SSDs [26]. By eliminating the need to involve the CPU for the bounce buffer, this approach enhances bandwidth and reduces both latency and CPU load.

Table 2 illustrates the key differences between earlier LLM systems supporting SSD offloading and TBA’s features:

Direct GPU–SSD data path. As Section 1 mentions, transfer via CPU interferes with CPU workloads, affecting efficiency.

	Flexgen	LLM in a Flash	ZeRO-Infinity	TBA
Training			✓	✓
Activation to main memory offloading to SSD	✓	✓	Checkpoints only	✓
Direct GPU–SSD data path				✓
Async data transfer				✓
Interoperability				✓

Table 2. Comparing TBA with other LLM systems providing SSD offloading features [1, 67, 75]. Without backward propagation, Inference systems may discard most intermediate tensors once a layer is done. We generalize “**Activation**” to refer to key-value (KV) cache in inference systems because it is reused across steps.

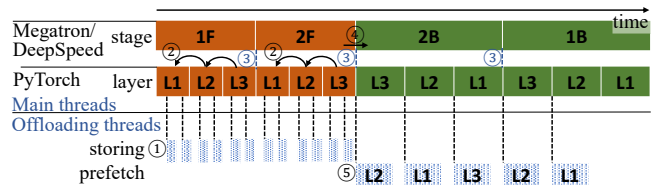


Figure 4. TBA timeline of a step of a 2-microbatch 3-layer (L) model. PyTorch hooks are used to trigger tensor cache bookkeeping, tensor offloading (①) and tensor loading (⑤). In the forward (F) propagation, TBA records the order of scopes (②) and switches between micro-batches at the end of the stages (③). TBA starts loading when it is switched to the backward (B) propagation (④).

Async data transfer. These systems either block the training computation when loading the offloaded data, or synchronize at each layer. Consequently, the I/O latency is exposed in the critical path. TBA hides the I/O latency by overlapping I/O with GPU computation.

Interoperability. Since LLM training requires a synergy of Python packages and the ecosystem is rapidly evolving, it is vital for the offloading feature to have good interoperability with other components in the same library or other libraries. TBA relies on process-local alternation to PyTorch execution and can work with distributed frameworks, such as Megatron and DeepSpeed. In contrast, DeepSpeed’s offloading features, e.g., ZeRO-Infinity, are available only in certain ZeRO stages. Flexgen and LLM in a Flash have their own runtime and do not work with distributed frameworks.

3 Design and Implementation

3.1 Overview of the TBA System

TBA implements a *tensor cache* to facilitate efficient offloading and reloading of tensors, facilitating the release of memory as well as the prefetch of tensors back to memory before they are needed for backward propagation. Figure 4

demonstrates how TBA works using PyTorch as an example. TBA launches its own threads (separate from PyTorch’s execution threads) to store tensors (①) and to load them back (⑤). In forward propagation (F), offloading of an activation starts once the operator producing it finishes (①). When activations are reused in backward propagation (B), prefetching (⑤) occurs in the reverse order of layers as recorded during forward propagation (②). When the last layer (L3 in the example) begins backward propagation, keeps the layer’s activations instead of offloading them (④). TBA keeps individual records for each micro-batch. Upon micro-batch changes (②), TBA switches its own record to the one corresponding to the new micro-batch.

Figure 5 shows the TBA software components. The tensor cache manages the activations and performs tensor offloading and loading. To achieve this, it uses PyTorch hooks to alter PyTorch execution. Section 3.2 details the design and implementation of the tensor cache. TBA has the SSD offloader that targets NVMe SSDs within the same node and the CPU offloader that targets host memory. Each offloader encapsulates the logic to transfer CUDA tensors to and from an offloading target. The SSD offloader leverages the GDS python binding, kvikio [54]. Using the LD_PRELOAD mechanism, CUDA malloc hook is a shared library that alters CUDA memory allocation and free API calls so that the memory is properly registered and deregistered for best GDS performance. This allows us to keep the PyTorch CUDA cached memory allocator for ease of comparison with baseline, without the need to replicate its implementation in a PyTorch pluggable memory allocator or modify the PyTorch runtime C++ code. The CPU offloader is for future work on clusters with massive remote SSD storage. It is backed by an allocator with pre-allocated host-pinned memory. The pool size is determined by profiling the first training step. New API calls are added to Megatron’s and DeepSpeed’s schedulers so that the tensor cache could get hints about stage changes and micro-batch changes, e.g., ③ and ④ in Figure 4. The next paragraph details hinted DeepSpeed’s scheduler as example.

To use TBA, moderate code additions are needed in the existing script: `configure_tensor_cache()` in Algorithm 1 shows the logic to configure tensor cache before training. The logic registers the PyTorch hooks, bookkeep the parameters to not offload them when they are registered onto the computation graph, and monkey-patch [89] the schedulers. With the dynamicity of PyTorch, monkey-patch overrides a defined function by assigning the custom implementation to the defined method in a package. `deepspeed_exec_schedule()` shows the hints added to DeepSpeed’s pipeline scheduler. Before and after execution, APIs are called to notify the tensor cache about the upcoming stage (Line 13) and the completion of an action (Line 15). Accordingly, the tensor cache can prefetch data, or wait I/O until it finishes. Megatron’s scheduler is patched similarly.

TBA extends naturally to distributed frameworks such as use with ZeRO, because frameworks such as DeepSpeed and Megatron divide the workload into processes built on top of PyTorch’s built-in tensor functionality. By working below PyTorch and keeping each process’ activities local, TBA applies directly to distributed launches.

3.2 Hook-Based Implementation of Tensor Cache

To benefit from tensor offloading, the GPU memory that the offloaded tensors own must be released when the tensors are not in use. However, PyTorch by default stores a reference to all the activations on the computation graph, disallowing the GPU memory to be reclaimed. The tensor cache alters the PyTorch execution so that the identifiers, not the references, of the activations are registered on the computation graph; upon PyTorch’s reusing the activation tensor, the tensor cache gets the identifier from the computation graph and use it as the key to return the requested tensor. In the forward propagation, when the tensor finishes offloading, the tensor cache no longer holds a reference to it, allowing its memory to be reclaimed by Python garbage collection once the Python control flow gets out of the function scope where the tensor object is used. In the backward propagation, the tensor cache holds a reference to the tensor by loading it from the SSD before its use; when all the module scopes the tensor is referred to have been finished, the reference is no longer held, allowing its memory to be reclaimed.

In short, the tensor cache is the in-memory structure that manages the references to all activations and keeps track of activations’ states, including whether they are being offloaded, the path in the file system, etc.

As Algorithm 2 shows, the tensor cache relies on the three PyTorch hook pairs to alter its execution behavior.

The forward hook pair works in the forward propagation: The start of a module triggers the forward pre hook, and the finish of a module triggers the forward hook. The tensor cache maintains the current scope stack using the forward hook pair: Upon entrance to a module, the module is pushed to the stack; When the module exits, it is popped out.

The backward hook pair is similar. When entering a module, the tensor cache prefetches activations in upcoming modules. Section 3.3.2 details prefetching. When exiting a module, the tensor cache removes it from the scope lists of all activations. Activations no longer in use are removed, whose memory will be released by garbage collection.

When a tensor is to be registered onto the computation graph, the pack hook is called to produce a value to be registered instead. When the tensor is reused, the unpack hooks is called to take in the object on the computation graph and return the original tensor. Figure 6 illustrates tensor cache’s activity when pack or unpack hook is triggered. When the multiply operator $x \cdot w$ finishes (①), the pack hook is called (②) on the input x and parameters w . Tensor cache has a

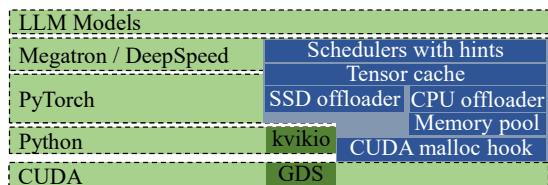


Figure 5. TBA software architecture. The components of TBA are shown as blue blocks. The CUDA malloc hook is a C++ library while others are Python code.

Algorithm 1: Logic to configure tensor cache before training and DeepSpeed scheduler logic with tensor cache hints. The original code before adding hints is blue. As shown, changes to adopt tensor cache are moderate.

Input: The tensor cache `tc` and the LLM model `model`.

```

1 Function configure_tensor_cache(tc, model):
2   tc.register_hooks()
3   for param in model.parameters():
4     | tc.register_parameters(param)
5   Monkey-patch DeepSpeed’s and Megatron’s schedulers.
6 Function deepspeed_exec_schedule(self, schedule):
7   for step_cmds in schedule:
8     for idx_cmd, cmd in enumerate(step_cmds):
9       tc.set_stage(cmd)
10      nxcmd = get_next(idx_cmd, step_cmds)
11      tc.set_next_stage(nxcmd)
12      if cmd is communication and nxcmd is backward pass:
13        | tc.prefetch_last_module()
14      self.execute(cmd)
15      if cmd is a backward pass: tc.wait_IO()

```

record of parameters, and accordingly returns `w` to let it registered on the graph as is. The tensor will also be returned as is if the tensor is on CPU or it is too small (Line 12 in Algorithm 2). As line 16 in Algorithm 2 shows, the tensor cache does not offload tensors but only keeps a record when the module is to be kept in the memory or in backward propagation. The first condition holds true when the adaptive offloading algorithm determines to keep the last few modules in GPU memory (Section 3.3.3). The second condition is true when an activation-checkpointing-enabled function does re-computation in the backward propagation to reproduce the activations. For tensor `x` in Figure 6, the tensor cache stores it to the SSDs (③), and returns a tensor identifier. When the unpack hook is triggered (Ⓑ), in the backward propagation (Ⓐ), the tensor cache either waits until the prefetch finishes (Ⓒ), and eventually returns the tensor.

3.3 Tensor Cache Mechanisms and Optimization

3.3.1 Deduplicating Tensors and Excluding Parameters. Tensor cache has a `get_id()` function to assign a unique identifier to each tensor. The shortcoming of PyTorch native `id()` is that its returned value is related to the GPU memory address. As TBA offloads activations, the latter will

be cleared by garbage collection once the control flow goes out of its use scope. The GPU memory address may be reused, causing identifier collision. To solve this, `get_id()` combines the timestamp when it first processes the tensor with the tensor shape as the unique identifier: When `get_id()` processes a tensor `t` for the first time, `get_id()` adds the current timestamp as an additional attribute to the tensor’s underlying storage `t.untyped_storage()` instead of `t`. This is because sometimes PyTorch creates new `torch.Tensor` objects representing the identical tensor. All future `get_id()` calls get the attribute value. This deduplicating scheme helps prevent redundant I/Os.

PyTorch registers all needed tensors in backward propagation into the computation graph, including activations and parameters. As this work focuses on offloading activations, the tensor cache excludes the model parameters. To achieve this, before training, the tensor cache records the identifiers of all model parameters (Line 4 in Algorithm 1). As linear layers store the transpose of the parameter tensors for backward propagation, the unique identifiers of the transpose are recorded. One benefit of our `get_id()` scheme is that the identifier for the transpose of the same parameter tensor remains consistent across steps. This is because the transpose uses the original tensor’s underlying storage, which we already assigned a timestamp to before training.

3.3.2 Offloading and Forwarding Tensors. The tensor cache has two thread pools—one for storing tensors and the other for loading tensors. The jobs submitted to each thread pool are executed in first-in-first-out (FIFO) order.

To hide the I/O latency, the tensor cache starts prefetching each activation before the corresponding module’s backward propagation. The activations in the last module is kept in GPU memory so they need not be prefetched. This simple scheme suffices because in PyTorch, CPU submits GPU kernel launches and memory operations ahead of GPU execution. Prefetching schemes are equivalent as long as there are always I/O tasks in GPU job queue to keep PCIe busy.

Upon loading a tensor, if it is still being stored, the tensor cache will return its original in-memory reference to skip loading from SSD. We call this data forwarding. For example, in Figure 6, when PyTorch engine retrieves tensor `x` from the MulBWD node, if it is still being stored to the SSDs, it is in memory. Instead of loading the tensor, the tensor cache returns its in-memory reference by converting the weak reference to a reference and store the obtained reference in the tensor cache for future if it is used in other scopes.

3.3.3 Adaptive Offloading. One insight we got during this work is that the activation offloading should target minimizing the peak memory usage, so that a configuration with larger activations could be accommodated by the same system without triggering out-of-memory (OOM) errors. Offloading tensors after the peak is not helpful. In Figure 7, the black curve is the memory footprint without offloading: it

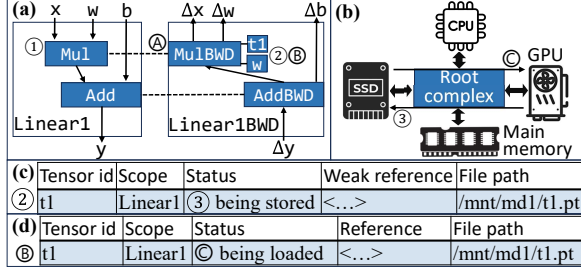


Figure 6. Tensor cache registers pack-unpack hook pair to offload tensors and reload tensors. (a) shows the PyTorch computation graph. (b) shows the hardware data path. (c) and (d) show the tensor cache state when the pack or unpack hook is triggered. During an operator (①), PyTorch calls the pack hook with tensors to be saved for backward propagation and registers the return values on the computation graph (②). Tensor cache tracks the tensors, offloads them (③), and returns identifiers for the tensors. In an operator (ⓐ) in the backward propagation, PyTorch calls the unpack hook with the identifiers to get tensors (ⓑ). The tensor cache blocks until the requested tensors are loaded in GPU memory (ⓒ).

Algorithm 2: Tensor cache registers PyTorch hooks to trigger actions during training.

Input: The tensor cache tc , current scope module, tensor to pack tensor, and/or object to unpack obj .

```

1 Function forward_pre_hook(module):
2   | Add module to  $tc$ 's current scope stack.
3 Function forward_hook(module):
4   | Pop  $tc$ 's innermost scope from the current scope stack.
5 Function full_backward_pre_hook*(module):
6   | Prefetch the tensors in the next module.
7 Function full_backward_hook*(module):
8   | for each tensor  $t$  in module tracked by  $tc$ :
9     |   Remove module from  $t$ 's record.
10    |   Release and stop tracking  $t$  if no scope is using  $t$ .
11 Function pack_hook(tensor):
12  | if  $tc.is\_parameter(tensor)$  or  $tensor.is\_cpu$  or
13  |    $math.prod(tensor.size()) < 2 * 20$ : return tensor
14  |    $tid = get\_id(tensor)$ 
15  |    $tc.add\_to\_current\_scope(tid)$ 
16  |   if  $tc.is\_current\_scope\_kept\_in\_memory()$  or
17  |    $tc.is\_current\_in\_backward()$ :
18  |     |  $tc.keep\_in\_gpu\_memory(tid, tensor)$ 
19  |   else:  $tc.offload(tid, tensor)$ 
20  |   return  $tid$ 
21 Function unpack_hook(obj):
22  | if  $isinstance(obj, torch.Tensor)$ : return  $obj$ 
23  |   if not  $tc.is\_loaded(obj)$ :  $tc.load\_or\_wait\_load(obj)$ 
24  |   return  $tc.get\_loaded\_tensor(obj)$ 

```

* PyTorch added `full_` prefix to the backward hook pair APIs to distinguish the current reworked design from the superseded one.

illustrates that GPU memory usage peaks at the beginning of the backward propagation. The blue curve shows the memory footprint with offloading, where the peak is delayed due

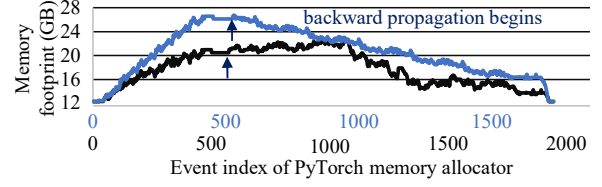


Figure 7. Memory footprint of one A100 in a BERT training step with offloading (black) and without (blue) on Table 3's system. Run with offloading incurs more allocator events because of memory release and allocation caused by tensor offloading and reloading. TBA reduces memory footprint at the beginning of backward propagation by 45% and end-to-end peak memory footprint by 25%.

Forward			
177.4ms, (415.1ms), 4.31GB			
To offload	Transformer 1	Transformer 2	To keep
	90.46 ms, 2.16 GB	58.90ms, 2.16GB	
Attention 1	MLP 1	Attention 2	MLP 2
28.37ms, 0.66GB	49.82ms, 0.94GB	15.60ms, 0.66GB	39.91ms, 0.94GB

Figure 8. The adaptive offloading algorithm uses profiling to decide modules in which the activations are to be kept in GPU memory. The model is represented as a tree where each scope is a node. On each node, the forward computation time and data transfer size are recorded during profiling. The I/O time in the forward propagation is also recorded and shown in parenthesis in the root node.

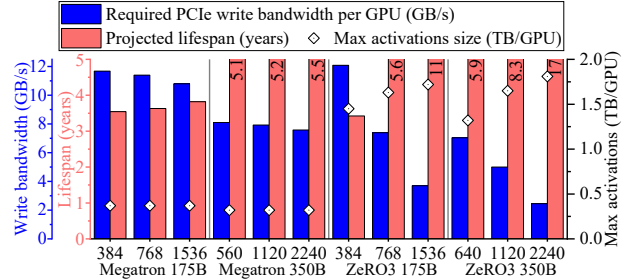


Figure 9. Estimate of SSD lifespan (left pink vertical axis), PCIe write bandwidth (left blue vertical axis) and maximal activations size per GPU (right vertical axis). Lifespans longer than 5 years are shown on top of the pink bars. The horizontal axis shows the number of GPUs, the framework and the model size [77]. ZeRO3 stands for DeepSpeed with stage-3 ZeRO, i.e., all of optimizer states, gradients, and parameters are sharded.

to the in-progress offloading jobs and new intermediate tensors created in the backward propagation. Excessive tensor offloading may keep the tensor reference even after its last use in the backward propagation, delaying the reclaim of its memory. To reduce unnecessary offloading after the peak, we devised adaptive offloading with two features.

First, when a thread is assigned a storing job, the thread will check if the tensor was forwarded. If so, the job will be canceled. Second, as illustrated by Figure 8, we devise an algorithm to choose a module from which the offloading is paused: we profile a step to collect (1) the data transfer

size and computation time of each MLP block and attention block, and (2) the forward propagation’s computation time, data transfer time, and total data transfer amount. Suppose module m is the last module to offload in a step. The required data transfer bandwidth is to finish offloading for all the modules before m and both offloading and reloading for module m by the time the backward propagation of module m begins. With the estimate that the backward propagation time is twice the forward propagation time, the required data transfer bandwidth can be calculated by the collected numbers and should be no larger than the write bandwidth in the measured forward propagation.

3.4 SSD Write Amount, Bandwidth, and Lifespan

To confirm if our design is viable in large-scale training systems, particularly concerning SSD endurance and required bandwidth, we conduct performance modeling to obtain forward propagation time per training step and the amount of activations produced in the process.

We extend the performance model package `llm-analysis` [39]. To estimate the forward propagation time, `llm-analysis` models each transformer layer as a simple pipeline, $t = \max(\sum_l \max(t_{l,compute}, t_{l,memory}), t_{ZeRO,communicate})$, where l denotes any layers inside a transformer layer. When ZeRO is enabled, the ZeRO communication time is assumed to be perfectly pipelined with the non-ZeRO computation and memory operations at the level of transformer layer.

We model the required PCIe write bandwidth per GPU as the total amount of activations divided by half the training time: As Section 3.3.3 explains, some of the activations may be written at the early stages of the backward propagation to reduce the needed PCIe bandwidth. We also assume that the training step time t_{step} is three times the forward propagation time. The lifespan is then projected as $t_{life} = S_{endurance} \cdot t_{step} / S_{activations}$ where $S_{endurance}$ is the lifetime writes allowed by the SSD endurance rating, $S_{activations}$ is the amount of activations per training step. We validated the $S_{activations}$ formula with profiled activations size in experiments in Section 4. We assume four Solidigm D7-P5810 12.8TB (Table 1) for each GPU, and assume the WAF is 2.5 in JESD rating and 1 in our scenario.

With these, we obtain Figure 9. We use the system configurations and measured floating points throughput from Megatron-LM [77]. The GPUs are A100 PCIe. Among all cases, the projected lifespan is more than 3 years, and the PCIe write bandwidth per GPU is no greater than 12.1GB/s. Moreover, when the system size and/or the model size scales up, the required PCIe write bandwidth reduces, and the projected lifespan increases. This effect occurs because larger systems imply increased communication overhead and reduced computation efficiency, thus slowing down training iterations on each GPU.

We also estimate the maximal activations size each GPU produces in one step: We compute the maximal micro-batch

size by assuming only two layers in a row are in GPU memory at the same time while all other activations are offloaded. Then, the activation maximal micro-batches produce in a step are the largest activations offloading could open up, which are shown as diamond marks in Figure 9. The maximal activations size per GPU ranges from 0.4 TB to 1.8 TB, while the micro-batch size ranges from 8 to 32. Activations so large can no longer be held by the main memory (Figure 2) and therefore SSD is the only choice as offloading target.

To further increase SSD endurance, the data retention period can be relaxed: NAND flash gets 50× PE cycles when the data retention period is relaxed from 3 years to 3 days [7, 33, 40]. This technique was not leveraged in the reasoning of this subsection, but we discuss its impact on cost in Section 4.4.

CPU	2× AMD EPYC 7702 64-core
Memory	DDR4-3200 1 TB
GPU	2× Nvidia A100 40 GB PCIe with NVLink
SSD	7× Intel Optane P5800X 1.6 TB. Two RAID0 arrays.
Software	Ubuntu 20.04.6 (kernel 5.15.0-113), CUDA 12.2 (driver 535.183.01), PyTorch 2.2.2, DeepSpeed 0.14.2, Megatron-DeepSpeed [46] (latest), kvikio 24.08

Table 3. Evaluation system configuration.

4 Evaluation

We evaluate TBA and answer the following questions.

- Q1. How well does TBA hide the I/O latency?
- Q2. How much is peak memory usage reduced by TBA?
- Q3. How much throughput boost can TBA deliver given the same per-GPU memory budget for activations?

Section 4.2 answers Q1 and Q2 by comparing TBA with execution without TBA. We discuss the performance analysis, impact of scaling up and cost in Section 4.4.

4.1 Experimental Setup

We use a machine with 2× A100 PCIe GPUs and 7× Intel P5800X SSDs, as Table 3 specifies. The SSDs are organized into two RAID0 arrays: one with 3 SSDs, and the other with 4 SSDs. We measured the memory use of the A100 with 4 SSDs during evaluation. Each array is the dedicated offloading target of one of the A100 GPUs. For consistent performance, the GPUs are locked at base frequency. The latest Megatron-DeepSpeed [46] is installed, which incorporates DeepSpeed techniques into Megatron and ensures interoperability.

We measure the system pretraining performance on three models, BERT [15] as an encoder-only model, GPT [64] as a decoder-only model, and T5 [65] as an encoder-decoder model. We use the OSCAR corpus [59, 60] as the dataset.

We use the two A100 GPUs for tensor parallelism. The number of micro-batches per step is fixed at 1 because without pipeline parallelism, in each training iteration, Megatron-DeepSpeed will not start a new micro-batch before both

forward propagation and backward propagation of the previous micro-batch are done. A micro-batch number larger than 1 only brings in gradient accumulation and does not make a difference in the activation offloading pattern. In our experiments, the hidden dimension is from 8192 to 16384, and we use typical hyperparameters [15, 65, 85] for hidden dimensions within this range. The attention head dimension is 128. The text sequence length is 1024. For T5, the number of decoders is half of the total number of layers, rounded down. FlashAttention-2 [11] is used with or without TBA for optimized attention computation.

As each A100 has only 40GB of device memory, to explore the design space closer to that in real-world training systems with A100 80GB and later GPUs [41, 77], we make several mitigations. First, we use FP16 precision instead of mixed precision, eliminating the FP32 weight copy. Second, we use SGD instead of Adam as the optimizer to reduce the memory use by optimizer states. The two measures only affect accumulation operations and gradient updates, thus imposing a constant bias in the training step time and memory usage in execution with or without TBA.

4.2 Performance and Peak Memory Usage

To understand TBA’s impact on execution time and peak memory usage, we measure the step time of BERT, T5, and GPT and the memory peak during forward and backward propagation. The collected metrics of system with TBA and without are compared in Figure 10. For each model, we collected three scenarios with different (hidden dimension, number of layers): (8192, 4), (12288, 3) and (16384, 2). As shown, TBA has almost no performance overhead in all cases. Although TBA and its optimizations introduce additional CPU-executed logic, the performance comparison indicates that this logic is not on the critical path. Rather, GPU computation defines the critical path, and the CPU’s role lies primarily in launching new GPU jobs before current GPU operations complete. Thus, the CPU is underutilized, and TBA’s extra work does not lead to delay in new tasks reaching the GPUs. In terms of the activations’ memory use, TBA effectively reduces the peak by 28%–40% in these cases.

4.3 Comparing the Activations Placement Strategies via Recompute-Offload-Keep (ROK) Curve

TBA opens up offloading activations to SSDs as an option besides keeping activations in the GPU memory, and activations checkpointing. We compare the three different strategies here by plotting the runs on the recompute-offload-keep (ROK) curve. Figure 11 shows the ROK curve for the training of two 3-layer BERT models, one with a hidden dimension of 12288 and the other with hidden dimension as 14336. In a ROK curve, each training run is represented by a point. The x-axis is the activations memory peak, and the y-axis is the model throughput. Model throughput [77] refers to the number of algorithmic computations involved in the training

step regardless of software and hardware implementation, e.g., whether the activations are recomputed, divided by the training step time. In these two cases, TBA reduces the GPU activations memory peak, allowing for a larger batch size to attain higher throughput. Given the same batch size, TBA offloading attains the throughput the same as the throughput when the activations are kept in memory. Meanwhile, TBA gets a lower activations memory peak than the recomputation. Compared with keeping the activations in memory, TBA is able to double the batch size with the same activations memory budget. Alternatively, people could leverage TBA to run a bigger model, or use fewer GPUs.

Other than the three strategies, before FlashAttention [12], Megatron [35] proposed selective recomputation: noting that in the transformer layer, the operations performed by the core attention module (the whole gray box in Figure 3) require less computation but create a large intermediate tensor when compared with the MLP block, the work recomputed only the core attention module. As we adopt FlashAttention, the core attention module is done in one kernel, eliminating these intermediate tensors. The effect of selective recomputation with FlashAttention has negligible impact on the performance and the peak memory usage for activations.

4.4 Discussion

Examining the modeling. To understand the accuracy of the performance model in Section 3.4, we compare the offloaded amount by TBA with the model estimate. As shown in Table 4, the figures are close. We also compute the required PCIe write bandwidth using half of the measured training time. As shown, when the hidden dimension gets larger, the PCIe write bandwidth is reduced. Typically, a model with more than 60b parameters has a hidden dimension of no less than 8k [29, 85]. The PCIe write bandwidth of the BERT models aligns with the estimate in Section 3.4.

	H8192 L4	H12288 L3	H16384 L2
Offloaded amount	10.37 GB	12.85 GB	10.75 GB
Model estimate	11.13 GB	12.6 GB	11.5 GB
PCIe write bandwidth	18.0 GB/s	13.8 GB/s	8.76 GB/s

Table 4. The offloaded tensor amount and model estimate when running BERT with different hidden dimensions (H) and number of layers (L). Batch size is 16. We also compute the PCIe write bandwidth required to fully offload the tensors.

Impact of upscaling. When LLM systems scale up, the computation efficiency decreases as a result of more cross-node communication. Section 2.2 demonstrates that the whole-system activations size $S_{activations}$ grows slower than the whole-system GPU throughput C , i.e., $S_{activations} \propto C^{\frac{5}{6}}$.

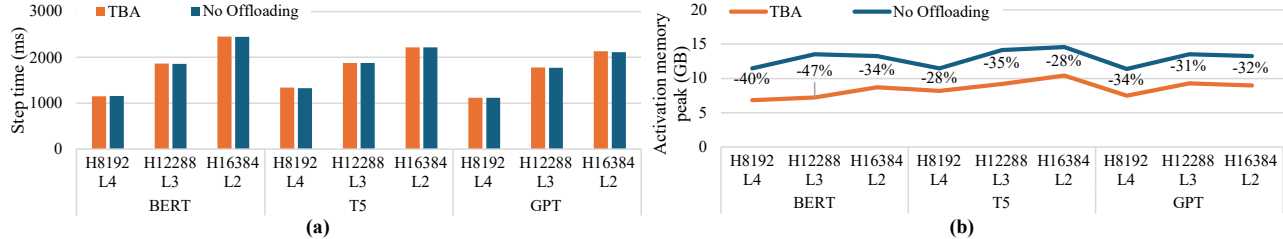


Figure 10. Comparing the step time and activations memory usage of TBA with execution without tensor offloading on BERT. We test several model configurations with different hidden dimensions (H) and number of layers (L). Batch size is 16.

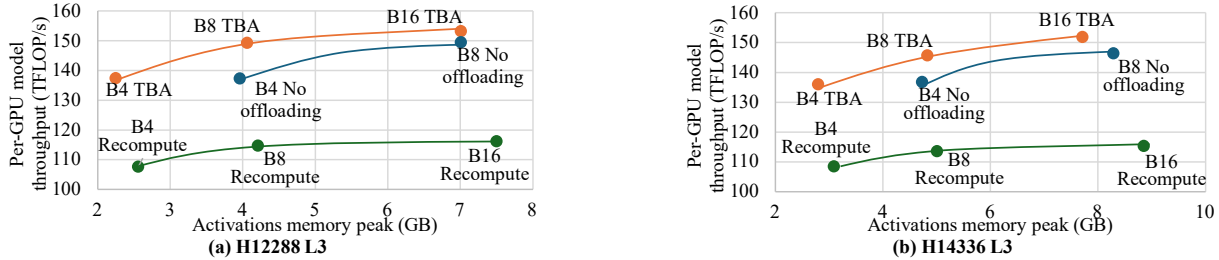


Figure 11. Recompute-offload-keep (ROK) curve of BERT with 3 layers (L) and hidden dimension (H) as (a) 12288 or (b) 14436. Designs with combination of different batch sizes (B), and choices to offload activations, keep activations, or recompute activations are shown.

Therefore, the bandwidth required to fully overlap the computation with the SSD accesses is reduced. In short, the scaling of LLM is essentially a weak scaling scenario, and the SSD IO latency is easier to hide when it is scaled up.

In a large-scale system, the larger amount of activations TBA allows to accommodate can be allocated to enlarge the number of microbatches and/or to enlarge the batch size. For example, pipeline parallelism brings about bubbles of idleness of the device, which could be mitigated by a larger number of microbatches [77]. Both the throughput boost by increased micro-batch size and that by increased number of micro-batches saturate at a point, leaving (1) the optimized strategy to allocate activations memory given parallelism configurations and (2) joint optimizations parallelism configurations and activations memory allocation open questions. We leave detailed throughput modeling of different parallelism strategies and microbatch sizes to future work.

Cost analysis. We study the SSD cost associated with adopting TBA offloading in LLM systems. To get the endurance in Figure 9, each A100 priced at US\$10k [16] is paired with in total US\$6.4k worth of SSDs. In the evaluation, we allocate 7 Intel P5800X for the 2 A100s. Although P5800X is more expensive than the models in Table 1, the price per PBW is comparable at US\$10.27 [52]. We can further reduce the cost to a few percentage by relaxing the data retention period. To have more durable storage for other data, the system may restrain the activation offloading to dedicated SSDs, or utilize hardware equipped with Zoned Namespaces (ZNS) standard [23, 83] to confine the wear within designated zones of physical blocks on the same SSD.

5 Related Work

Swapping and offloading. Many LLM systems with offloading abilities are inference-only [1, 36, 75]. In inference, weights and KV-cache never change and are reused across iterations; Researchers leverage this to enhance locality and memory efficiency. However, in LLM training, the weights are updated in each iteration and all tensors change across the iterations. Some work avails offloading feature [67] for training, but are mostly designed to accommodate larger models in a smaller system at the cost of performance. They lack the async data transfer ability to maintain performance.

Another direction is to offload data and the associated computation to the CPU [30, 69, 82]. The offloaded computation is relatively light, and the offloaded data include gradients, sparse elements in the weights, etc. Recognizing this direction, our work is made orthogonal because we offload the activations to SSDs via GDS to minimize the interference with the CPU. Activations are for gradient computation, which is compute-intensive and best done solely on GPUs.

Before the massive adoption of LLMs, there is work on offloading data for deep learning [5, 24, 61, 70, 87]. Most of them offload data to main memory while some [5] enable the GPU-SSD data path. LLM training is unique because massive parallelism and its implications on the memory use of optimizer states, gradients, and weights are fundamental to the design space. TBA naturally supports multiple GPUs. Besides, we demonstrated its viability on clusters and introduced the ROK curve to help design choice. On the other hand, LLM has such a high demand for computing power that it stimulates rapid development in specialized hardware, e.g.,

transformer engine [55], and distributed framework. This is why we ensure good interoperability. Most earlier work in this direction is, in contrast, bound to a specific PyTorch version or a custom runtime with support to select layers.

Quantization and sparsity. Some work on offloading use quantization and/or sparsity to reduce the I/O size [1, 5, 75]. To reduce computation, algorithms have been proposed to quantize parameters and introduce sparsity into the model [14, 18, 32, 42, 92]. Mixture-of-Experts (MoE) [74] is in this direction as it sparsifies the token-to-neuron connection in the MLP to token-to-expert connection. Some algorithms introduce structured sparsity, e.g., N:M [94] sparsity and 2:4 [62] sparsity. On the other hand, there are frameworks and specialized kernels to accelerate models with quantization and/or sparsity [19, 20, 76, 93]. Some kernels leverage specialized hardware, e.g., Ampere tensor core [10, 50]. These techniques are orthogonal to our work and can be used to alternate the model and accelerate the computation while using TBA. Notably, given the hardware, the reuse factor to fully overlap the computation with PCIe transfer will change according to the new numerical format or sparsity access pattern. We believe TBA’s adaptive offloading algorithm helps optimize the offload amounts in these cases.

Optimized kernels. Previous work develops optimized kernels to accelerate LLM [11, 12, 56]. Some kernels utilize special hardware [57]. TBA’s interoperability ensures it can be used easily with these and upcoming techniques.

6 Conclusion

In LLM training systems, activations dominates the increasingly limited GPU memory. We propose TBA to address this by offloading activations to SSDs. We demonstrate its viability in large-scale systems by modeling. We incorporate into TBA a direct GPU-SSD data path and good interoperability. To fully overlap computation with data transfer, TBA features async data transfer, tensor deduplication, forwarding, and adaptive offloading. Evaluation shows TBA reduces the activations peak memory use by up to 47% with negligible overhead. We introduce the ROK curve to show advantages of TBA’s offloading over recomputation and keeping activations in memory.

References

- [1] Keivan Alizadeh, Iman Mirzadeh, Dmitry Belenko, Karen Khatamifard, Minsik Cho, Carlo C. Del Mundo, Mohammad Rastegari, and Mehrdad Farajtabar. 2024. LLM in a Flash: Efficient Large Language Model Inference with Limited Memory. arXiv:2312.11514 [cs]
- [2] Reza Yazdani Aminabadi, Samyam Rajbhandari, Minjia Zhang, Ammar Ahmad Awan, Cheng Li, Du Li, Elton Zheng, Jeff Rasley, Shaden Smith, Olatunji Ruwase, and Yuxiong He. 2022. DeepSpeed Inference: Enabling Efficient Inference of Transformer Models at Unprecedented Scale. arXiv:2207.00032 [cs]
- [3] Jason Ansel, Edward Yang, Horace He, Natalia Gimelshein, Animesh Jain, Michael Voznesensky, Bin Bao, Peter Bell, David Berard, Evgeni Burovski, Geeta Chauhan, Anjali Chourdia, Will Constable, Alban Desmaison, Zachary DeVito, Elias Ellison, Will Feng, Jiong Gong, Michael Gschwind, Brian Hirsh, Sherlock Huang, Kshiteej Kalambarakar, Laurent Kirsch, Michael Lazos, Mario Lezcano, Yanbo Liang, Jason Liang, Yinghai Lu, C. K. Luk, Bert Maher, Yunjie Pan, Christian Puhersch, Matthias Reso, Mark Saroufim, Marcos Yukio Siraichi, Helen Suk, Shunting Zhang, Michael Suo, Phil Tillet, Xu Zhao, Eikan Wang, Keren Zhou, Richard Zou, Xiaodong Wang, Ajit Mathews, William Wen, Gregory Chanan, Peng Wu, and Soumith Chintala. 2024. PyTorch 2: Faster Machine Learning Through Dynamic Python Bytecode Transformation and Graph Compilation. In *Proceedings of the 29th ACM International Conference on Architectural Support for Programming Languages and Operating Systems, Volume 2* (La Jolla CA USA, 2024-04-27). ACM, 929–947. <https://doi.org/10.1145/3620665.3640366>
- [4] Quentin Anthony, Jacob Hatfield, Deepak Narayanan, Stella Biderman, Stas Bekman, Junqi Yin, Aamir Shafi, Hari Subramoni, and Dhaleswar Panda. 2024. The Case for Co-Designing Model Architectures with Hardware. arXiv:2401.14489 [cs]
- [5] Jonghyun Bae, Jongsung Lee, Yunho Jin, Sam Son, Shine Kim, Tae Jun Ham, Jae W Lee, and Hakbeom Jang. 2021. FlashNeuron: SSD-Enabled Large-Batch Training of Very Deep Neural Networks. In *Proceedings of the 19th USENIX Conference on File and Storage Technologies* (Virtual Event, 2021-02-23).
- [6] Tom B. Brown, Benjamin Mann, Nick Ryder, Melanie Subbiah, Jared Kaplan, Prafulla Dhariwal, Arvind Neelakantan, Pranav Shyam, Girish Sastry, Amanda Askell, Sandhini Agarwal, Ariel Herbert-Voss, Gretchen Krueger, Tom Henighan, Rewon Child, Aditya Ramesh, Daniel M. Ziegler, Jeffrey Wu, Clemens Winter, Christopher Hesse, Mark Chen, Eric Sigler, Mateusz Litwin, Scott Gray, Benjamin Chess, Jack Clark, Christopher Berner, Sam McCandlish, Alec Radford, Ilya Sutskever, and Dario Amodei. 2020. Language Models are Few-Shot Learners. arXiv:2005.14165 [cs.CL] <https://arxiv.org/abs/2005.14165>
- [7] Yu Cai, Gulay Yalcin, Onur Mutlu, Erich F. Haratsch, Adrian Cristal, Osman S. Unsal, and Ken Mai. 2012. Flash Correct-and-Refresh: Retention-aware Error Management for Increased Flash Memory Lifetime. In *2012 IEEE 30th International Conference on Computer Design (ICCD)* (2012-09), 94–101. <https://doi.org/10.1109/ICCD.2012.6378623>
- [8] Lequn Chen. 2023. Dissecting Batching Effects in GPT Inference. <https://le.qun.ch/en/blog/2023/05/13/transformer-batching/>. Accessed 07/21/2024.
- [9] Tianqi Chen, Bing Xu, Chiyuan Zhang, and Carlos Guestrin. 2016. Training Deep Nets with Sublinear Memory Cost. arXiv:1604.06174 [cs]
- [10] Zhaodong Chen, Zheng Qu, Yuying Quan, Liu Liu, Yufei Ding, and Yuan Xie. 2023. Dynamic N:M Fine-Grained Structured Sparse Attention Mechanism. In *Proceedings of the 28th ACM SIGPLAN Annual Symposium on Principles and Practice of Parallel Programming* (New York, NY, USA, 2023-02-21) (PPoPP ’23). Association for Computing Machinery, 369–379. <https://doi.org/10.1145/3572848.3577500>
- [11] Tri Dao. 2023. FlashAttention-2: Faster Attention with Better Parallelism and Work Partitioning. <https://doi.org/10.48550/arXiv.2307.08691> arXiv:2307.08691 [cs]
- [12] Tri Dao, Daniel Y. Fu, Stefano Ermon, Atri Rudra, and Christopher Ré. 2022. FlashAttention: Fast and Memory-Efficient Exact Attention with IO-Awareness. <https://doi.org/10.48550/arXiv.2205.14135> arXiv:2205.14135 [cs]
- [13] David Meyer. 2024. *The Cost of Training AI Could Soon Become Too Much to Bear*. Yahoo Finance. <https://finance.yahoo.com/news/cost-training-ai-could-soon-101348308.html>
- [14] Tim Dettmers, Ruslan Svirschevski, Vage Egiazarian, Denis Kuznedelev, Elias Frantar, Saleh Ashkboos, Alexander Borzunov, Torsten Hoefer, and Dan Alistarh. 2023. SpQR: A Sparse-Quantized Representation for Near-Lossless LLM Weight Compression. <https://doi.org/10.48550/arXiv.2306.03078> arXiv:2306.03078 [cs]

- [15] Jacob Devlin, Ming-Wei Chang, Kenton Lee, and Kristina Toutanova. 2019. BERT: Pre-training of Deep Bidirectional Transformers for Language Understanding. <https://doi.org/10.48550/arXiv.1810.04805> arXiv:1810.04805 [cs]
- [16] Dihuni. 2021. NVIDIA A100 900-21001-0000-000 40GB Ampere PCIe GPU for Deep Learning AI, HPC, Analytics and Research – Dihuni – GPU Server for AI, Data Center & IoT Hardware & Software Solutions. <https://www.dihuni.com/product/nvidia-a100-900-21001-0000-000-40gb-ampere-pcie-gpu-for-deep-learning/>
- [17] Dihuni. 2024. SOLIDIGM SSDPF2SQ800GZ01 D7-P5810 Solid State Drive – Dihuni – GPU Server for AI, Data Center & IoT Hardware & Software Solutions. <https://www.dihuni.com/product/solidigm-ssdpf2sq800gz01-d7-p5810-solid-state-drive/>. Accessed 07/21/2024.
- [18] Elias Frantar and Dan Alistarh. 2023. SparseGPT: Massive Language Models Can Be Accurately Pruned in One-Shot. In *Proceedings of the 40th International Conference on Machine Learning (Honolulu, Hawaii, USA, 2023-07-23) (ICML '23)*. JMLR.org. <https://doi.org/10.5555/3618408.3618822>
- [19] Trevor Gale, Deepak Narayanan, Cliff Young, and Matei Zaharia. 2023. MegaBlocks: Efficient Sparse Training with Mixture-of-Experts. In *Proceedings of Machine Learning and Systems 5 (MLSys 2023) (2023)*, Vol. 5. Curran, 288–304. arXiv:2211.15841 [cs] https://proceedings.mlsys.org/paper_files/paper/2023/file/5a54f79333768effe7e8927bcccfe40-Paper-mlsys2023.pdf
- [20] Trevor Gale, Matei Zaharia, Cliff Young, and Erich Elsen. 2020. Sparse GPU Kernels for Deep Learning. In *SC20: International Conference for High Performance Computing, Networking, Storage and Analysis (Atlanta, GA, USA, 2020-11)*. IEEE, 1–14. <https://doi.org/10.1109/SC41405.2020.00021>
- [21] Google. 2017. GPU Machine Types | Compute Engine Documentation. <https://cloud.google.com/compute/docs/gpus>. Accessed 07/21/2024.
- [22] Google. 2022. About Google Cloud Hyperdisk | Compute Engine Documentation. <https://cloud.google.com/compute/docs/disks/hyperdisks>. Accessed 07/30/2024.
- [23] Kyuhwa Han, Hyunho Gwak, Dongkun Shin, and Joo-Young Hwang. 2021. ZNS+: Advanced Zoned Namespace Interface for Supporting In-Storage Zone Compaction. In *Proceedings of the 15th USENIX Symposium on Operating Systems Design and Implementation (Virtual Event, 2021-07-14)*. 147–162.
- [24] Chien-Chin Huang, Gu Jin, and Jinyang Li. 2020. SwapAdvisor: Pushing Deep Learning Beyond the GPU Memory Limit via Smart Swapping. In *Proceedings of the Twenty-Fifth International Conference on Architectural Support for Programming Languages and Operating Systems*. ACM, Lausanne Switzerland, 1341–1355. <https://doi.org/10.1145/3373376.3378530>
- [25] Intel. 2018. Over-Provisioning NAND-Based Intel® SSDs for Better Endurance. <https://www.ioncomputer.com/ion/body/documents/over-provisioning-nand-based-ssds-better-endurance-whitepaper.pdf>
- [26] Devasena Inupakutika, Bridget Davis, Qirui Yang, Daniel Kim, and David Akopian. 2022. Quantifying Performance Gains of GPUDirect Storage. In *2022 IEEE International Conference on Networking, Architecture and Storage (NAS) (2022-10)*. 1–9. <https://doi.org/10.1109/NAS55553.2022.9925516>
- [27] JEDEC SOLID STATE TECHNOLOGY ASSOCIATION. 2016. JESD218B: Solid-State Drive (SSD) Requirements and Endurance Test Method. <https://www.jedec.org/sites/default/files/docs/JESD218B.pdf>
- [28] Ziheng Jiang, Haibin Lin, Yinmin Zhong, Qi Huang, Yangrui Chen, Zhi Zhang, Yanghua Peng, Xiang Li, Cong Xie, Shibiao Nong, Yulu Jia, Sun He, Hongmin Chen, Zhihao Bai, Qi Hou, Shipeng Yan, Ding Zhou, Yiyao Sheng, Zhuo Jiang, Haohan Xu, Haoran Wei, Zhang Zhang, Pengfei Nie, Leqi Zou, Sida Zhao, Liang Xiang, Zherui Liu, Zhe Li, Xiaoying Jia, Jianxi Ye, Xin Jin, and Xin Liu. 2024. MegaScale: Scaling Large Language Model Training to More Than 10,000 GPUs. arXiv:2402.15627 [cs]
- [29] Jordan Hoffmann, Sebastian Borgeaud, Arthur Mensch, Elena Buchatskaya, Trevor Cai, Eliza Rutherford, Diego de Las Casas, Lisa Anne Hendricks, Johannes Welbl, Aidan Clark, Tom Hennigan, Eric Noland, Katie Millican, George Driessche, Bogdan Damoc, Aurelia Guy, Simon Osindero, Karen Simonyan, Erich Elsen, Jack W. Rae, Oriol Vinyals, and Laurent Sifre. 2022. *Training Compute-Optimal Large Language Models*. arXiv:2203.15556 [cs] <http://arxiv.org/abs/2203.15556>
- [30] Keisuke Kamahori, Yile Gu, Kan Zhu, and Baris Kasikci. 2024. *Fiddler: CPU-GPU Orchestration for Fast Inference of Mixture-of-Experts Models*. <https://doi.org/10.48550/arXiv.2402.07033> arXiv:2402.07033 [cs]
- [31] Jared Kaplan, Sam McCandlish, Tom Henighan, Tom B. Brown, Benjamin Chess, Rewon Child, Scott Gray, Alec Radford, Jeffrey Wu, and Dario Amodei. 2020. Scaling Laws for Neural Language Models. arXiv:2001.08361 [cs, stat]
- [32] Sehoon Kim, Coleman Hooper, Amir Gholami, Zhen Dong, Xiuyu Li, Sheng Shen, Michael W. Mahoney, and Kurt Keutzer. 2024. *SqueezeLLM: Dense-and-Sparse Quantization*. <https://doi.org/10.48550/arXiv.2306.07629> arXiv:2306.07629 [cs]
- [33] Shine Kim, Yunho Jin, Gina Sohn, Jonghyun Bae, Tae Jun Ham, and Jae W. Lee. 2021. Behemoth: A Flash-centric Training Accelerator for Extreme-scale {DNNs}. 371–385. <https://www.usenix.org/conference/fast21/presentation/kim>
- [34] KIOXIA. 2022. FL6 Series (2.5-Inch) | KIOXIA - United States (English). <https://americas.kioxia.com/en-us/business/ssd/enterprise-ssd/fl6.html>. Accessed 07/21/2024.
- [35] Vijay Korthikanti, Jared Casper, Sangkug Lym, Lawrence McAfee, Michael Andersch, Mohammad Shoeybi, and Bryan Catanzaro. 2022. Reducing Activation Recomputation in Large Transformer Models. <https://doi.org/10.48550/arXiv.2205.05198> arXiv:2205.05198 [cs]
- [36] Woosuk Kwon, Zhuohan Li, Siyuan Zhuang, Ying Sheng, Lianmin Zheng, Cody Hao Yu, Joseph Gonzalez, Hao Zhang, and Ion Stoica. 2023. Efficient Memory Management for Large Language Model Serving with PagedAttention. In *Proceedings of the 29th Symposium on Operating Systems Principles (Koblenz Germany, 2023-10-23)*. ACM, 611–626. <https://doi.org/10.1145/3600006.3613165>
- [37] LangChain. 2022. *LangChain*. <https://github.com/langchain-ai/langchain>
- [38] Lenovo. 2023. *What Do I Need to Know about SSD Endurance and Overprovisioning?* <https://thinksystem.lenovofiles.com/storage/help/index.jsp?topic=%2Fde-series-olh-11.80%2Fwhat-do-i-need-to-know-about-ssd-endurance-and-overprovisioning.html>
- [39] Cheng Li. 2023. LLM-Analysis: Latency and Memory Analysis of Transformer Models for Training and Inference. <https://github.com/cli99/llm-analysis>. Accessed 07/04/2024.
- [40] Ren-Shuo Liu, Chia-Lin Yang, and Wei Wu. 2012. Optimizing NAND Flash-Based SSDs via Retention Relaxation. In *10th USENIX Conference on File and Storage Technologies (FAST 12) (San Jose, CA, 2012)*. USENIX Association.
- [41] Zirui Liu, Guanchu Wang, Shaochen Zhong, Zhaozhuo Xu, Daochen Zha, Ruixiang Tang, Zhimeng Jiang, Kaixiong Zhou, Vipin Chaudhary, Shuai Xu, and Xia Hu. 2023. Winner-Take-All Column Row Sampling for Memory Efficient Adaptation of Language Model. arXiv:2305.15265 [cs]
- [42] Zichang Liu, Jue Wang, Tri Dao, Tianyi Zhou, Binhang Yuan, Zhao Song, Anshumali Shrivastava, Ce Zhang, Yuandong Tian, Christopher Ré, and Beidi Chen. 2023. Deja Vu: Contextual Sparsity for Efficient LLMs at Inference Time. In *Proceedings of the 40th International Conference on Machine Learning (Honolulu, Hawaii, USA, 2023-07-23) (ICML '23)*. JMLR.org. <https://doi.org/10.5555/3618408.3619327>
- [43] Glenn K. Lockwood, Alberto Chiusole, Lisa Gerhardt, Kirill Lozinskiy, David Paul, and Nicholas J. Wright. 2024. Architecture and Performance of Perlmutter’s 35 PB ClusterStor E1000 All-flash File System. *Concurrency and Computation: Practice and Experience* (2024), e8143.

- <https://doi.org/10.1002/cpe.8143>
- [44] Stathis Maneas, Kaveh Mahdaviyani, Tim Emami, and Bianca Schroeder. 2022. Operational Characteristics of SSDs in Enterprise Storage Systems: A Large-Scale Field Study. In *Proceedings of the 20th USENIX Conference on File and Storage Technologies* (SANTA CLARA, CA, 2022-02-22).
- [45] Sam McCandlish, Jared Kaplan, Dario Amodei, and OpenAI Dota Team. 2018. An Empirical Model of Large-Batch Training. arXiv:1812.06162 [cs, stat]
- [46] Microsoft. 2019. *Microsoft/Megatron-DeepSpeed: Ongoing Research Training Transformer Language Models at Scale, Including: BERT & GPT-2*. <https://github.com/microsoft/Megatron-DeepSpeed>
- [47] Microsoft. 2023. *Bing Chat | Microsoft Edge*. <https://www.microsoft.com/en-us/edge/features/bing-chat>
- [48] Microsoft. 2024. ND A100 V4-Series - Azure Virtual Machines. <https://learn.microsoft.com/en-us/azure/virtual-machines/nda100-v4-series>. Accessed 07/21/2024.
- [49] Midjourney. 2022. *Midjourney*. <https://www.midjourney.com/website>
- [50] Asit Mishra, Jorge Albericio Latorre, Jeff Pool, Darko Stosic, Dusan Stosic, Ganesh Venkatesh, Chong Yu, and Paulius Micikevicius. 2021. *Accelerating Sparse Deep Neural Networks*. arXiv:2104.08378 [cs] <http://arxiv.org/abs/2104.08378>
- [51] NCSA. 2022. Delta Project Profile. <https://www.ncsa.illinois.edu/research/project-highlights/delta/>. Accessed 07/21/2024.
- [52] Newegg. 2021. *Intel Optane DC P5800X Series 1.6TB, 2.5" x 15mm, U.2, PCIe 4.0 X4, 3D XPoint Solid State Drive (SSD) SSDPF21Q016TB01 - Newegg.Com*. https://www.newegg.com/intel-optane-ssd-dc-p5800x-1-6tb/p/N82E16820167481?item=N82E16820167481&nm_mc=knc-googleleadwords&cm_mmc=knc-googleleadwords_-_solid%20state%20disk%20-%20enterprise_-_intel_-_20167481&utm_source=google&utm_medium=organic+shopping&utm_campaign=knc-googleleadwords_-_solid%20state%20disk%20-%20enterprise_-_intel_-_20167481&source=region
- [53] Newegg. 2024. *Solidigm™ Solid State Drive D7-P5620 Series (12.8TB, U.2 15mm, 2.5", PCIe 4.0 X4, 3D4, TLC) Generic No OPAL Single Pack Data Center / Server / Internal SSD (SSDPF2KE128T1N1) - Newegg.Com*. <https://www.newegg.com/solidigm-12-8-tb-d7-p5620-series/p/N82E16820318023>. Accessed 07/21/2024.
- [54] Nvidia. 2022. *Rapidsai/Kvikio: Kvikio - High Performance File IO*. <https://github.com/rapidsai/kvikio>. Accessed 07/21/2024.
- [55] Nvidia. 2023. *NVIDIA H100 Tensor Core GPU Architecture*. <https://resources.nvidia.com/en-us-tensor-core?ncid=no-ncid>
- [56] Nvidia. 2023. *NVIDIA/TensorRT-LLM*. <https://github.com/NVIDIA/TensorRT-LLM>
- [57] Nvidia. 2023. *NVIDIA/TransformerEngine*. <https://github.com/NVIDIA/TransformerEngine>
- [58] OpenAI. 2022. *ChatGPT*. <https://chatgpt.com/>
- [59] Pedro Javier Ortiz Su'arez, Laurent Romary, and Benoit Sagot. 2020. A Monolingual Approach to Contextualized Word Embeddings for Mid-Resource Languages. In *Proceedings of the 58th Annual Meeting of the Association for Computational Linguistics*. Association for Computational Linguistics, Online, 1703–1714. <https://www.aclweb.org/anthology/2020.acl-main.156>
- [60] Pedro Javier Ortiz Su'arez, Benoit Sagot, and Laurent Romary. 2019. Asynchronous pipelines for processing huge corpora on medium to low resource infrastructures (*Proceedings of the Workshop on Challenges in the Management of Large Corpora (CMC-7) 2019, Cardiff, 22nd July 2019*), Piotr Bański, Adrien Barbaresi, Hanno Biber, Evelyn Breiteneder, Simon Clematide, Marc Kupietz, Harald L"ungen, and Caroline Iliadi (Eds.). Leibniz-Institut f"ur Deutsche Sprache, Mannheim, 9 – 16. <https://doi.org/10.14618/ids-pub-9021>
- [61] Xuan Peng, Xuanhua Shi, Hulin Dai, Hai Jin, Weiliang Ma, Qian Xiong, Fan Yang, and Xuehai Qian. 2020. Capuchin: Tensor-based GPU Memory Management for Deep Learning. In *Proceedings of the Twenty-Fifth International Conference on Architectural Support for Programming Languages and Operating Systems*. ACM, Lausanne Switzerland, 891–905. <https://doi.org/10.1145/3373376.3378505>
- [62] Jeff Pool and Chong Yu. 2021. Channel Permutations for N:M Sparsity. In *Advances in Neural Information Processing Systems* (2021), Vol. 34. Curran Associates, Inc., 13316–13327. https://proceedings.neurips.cc/paper_files/paper/2021/hash/6e8404c3b93a9527c8db241a1846599a-Abstract.html
- [63] QNAP Systems, Inc. 2018. QNAP NAS Solution: QTS SSD Extra Over-Provisioning. <https://anfatech.com.vn/wp-content/uploads/2021/03/ssd-over-provisioning.pdf>
- [64] Alec Radford, Jeffrey Wu, Rewon Child, David Luan, Dario Amodei, and Ilya Sutskever. 2019. *Language Models Are Unsupervised Multitask Learners*. https://d4mucfpsyw.cloudfront.net/better-language-models/language_models_are_unsupervised_multitask_learners.pdf
- [65] Colin Raffel, Noam Shazeer, Adam Roberts, Katherine Lee, Sharan Narang, Michael Matena, Yanqi Zhou, Wei Li, and Peter J. Liu. 2023. Exploring the Limits of Transfer Learning with a Unified Text-to-Text Transformer. <https://doi.org/10.48550/arXiv.1910.10683> arXiv:1910.10683 [cs, stat]
- [66] Samyam Rajbhandari, Jeff Rasley, Olatunji Ruwase, and Yuxiong He. 2020. ZeRO: Memory Optimizations Toward Training Trillion Parameter Models. In *SC20: International Conference for High Performance Computing, Networking, Storage and Analysis*. IEEE, Atlanta, GA, USA, 1–16. <https://doi.org/10.1109/SC41405.2020.00024>
- [67] Samyam Rajbhandari, Olatunji Ruwase, Jeff Rasley, Shaden Smith, and Yuxiong He. 2021. ZeRO-infinity: Breaking the GPU Memory Wall for Extreme Scale Deep Learning. In *Proceedings of the International Conference for High Performance Computing, Networking, Storage and Analysis*. ACM, St. Louis Missouri, 1–14. <https://doi.org/10.1145/3458817.3476205>
- [68] Jeff Rasley, Samyam Rajbhandari, Olatunji Ruwase, and Yuxiong He. 2020. DeepSpeed: System Optimizations Enable Training Deep Learning Models with Over 100 Billion Parameters. In *Proceedings of the 26th ACM SIGKDD International Conference on Knowledge Discovery & Data Mining*. ACM, Virtual Event CA USA, 3505–3506. <https://doi.org/10.1145/3394486.3406703>
- [69] Jie Ren, Samyam Rajbhandari, Reza Yazdani Aminabadi, Shuangyan Yang, Minjia Zhang, Dong Li, Olatunji Ruwase, and Yuxiong He. 2021. ZeRO-Offload: Democratizing Billion-Scale Model Training. In *Proceedings of the 2021 USENIX Annual Technical Conference* (Virtual Event, 2021).
- [70] Minsoo Rhu, Natalia Gimelshein, Jason Clemons, Arslan Zulfiqar, and Stephen W. Keckler. 2016. vDNN: Virtualized Deep Neural Networks for Scalable, Memory-Efficient Neural Network Design. arXiv:1602.08124 [cs]
- [71] Samsung. 2017. Ultra-Low Latency with Samsung Z-NAND SSD. <https://download.semiconductor.samsung.com/resources/brochure/Ultra-LowLatencywithSamsungZ-NANDSSD.pdf>. Accessed 07/30/2024.
- [72] Samsung. 2019. Over-Provisioning Benefits for Samsung Data Center SSDs. <https://download.semiconductor.samsung.com/resources/white-paper/S190311-SAMSUNG-Memory-Over-Provisioning-White-paper.pdf>
- [73] ServerOrbit. 2024. Kioxia FL6XHUL1T60 1.6TB PCIe4 NVMe SSD Brand New. <https://serverorbit.com/buy-kioxia-fl6xhul1t60-1-6tb-pcie4-nvme-ssd/>. Accessed 07/21/2024.
- [74] Noam Shazeer, Azalia Mirhoseini, Krzysztof Maziarz, Andy Davis, Quoc Le, Geoffrey Hinton, and Jeff Dean. 2017. *Outrageously Large Neural Networks: The Sparsely-Gated Mixture-of-Experts Layer*. <https://doi.org/10.48550/arXiv.1701.06538> arXiv:1701.06538 [cs, stat]

- [75] Ying Sheng, Lianmin Zheng, Binhang Yuan, Zhuohan Li, Max Ryabinin, Daniel Y. Fu, Zhiqiang Xie, Beidi Chen, Clark Barrett, Joseph E. Gonzalez, Percy Liang, Christopher Ré, Ion Stoica, and Ce Zhang. 2023. FlexGen: High-Throughput Generative Inference of Large Language Models with a Single GPU. arXiv:2303.06865 [cs]
- [76] Shigang Li, Kazuki Osawa, and Torsten Hoefler. 2021. Efficient Quantized Sparse Matrix Operations on Tensor Cores. In *Proceedings of the International Conference on High Performance Computing, Networking, Storage and Analysis* (Dallas, Texas, 2024-07-17T07:20:44Z) (SC'22). IEEE Press. <https://github.com/Shigangli/Magicube>
- [77] Mohammad Shoeybi, Mostafa Patwary, Raul Puri, Patrick LeGresley, Jared Casper, and Bryan Catanzaro. 2020. Megatron-LM: Training Multi-Billion Parameter Language Models Using Model Parallelism. <https://doi.org/10.48550/arXiv.1909.08053> arXiv:1909.08053 [cs]
- [78] SMART Modular Technologies, Inc. 2024. *Why SMART's Over-Provisioning?* <https://www.smartm.com/technology/over-provisioning>
- [79] Solidigm. 2022. *Solidigm™ SSD Endurance Estimator*. <https://estimator.solidigm.com/ssdendurance/index.htm>
- [80] Solidigm. 2023. D7-P5620 Mid-Endurance PCIe 4.0 NVMe SSD for Data Centers | Solidigm D7 SSD. <https://www.solidigm.com/products/data-center/d7/p5620.html>. Accessed 07/21/2024.
- [81] Solidigm. 2023. D7-P5810. <https://www.solidigm.com/products/data-center/d7/p5810.html>. Accessed 07/21/2024.
- [82] Yixin Song, Zeyu Mi, Haotong Xie, and Haibo Chen. 2023. *PowerInfer: Fast Large Language Model Serving with a Consumer-grade GPU*. arXiv:2312.12456 [cs] <http://arxiv.org/abs/2312.12456>
- [83] Theano Stavrinou, Daniel S. Berger, Ethan Katz-Bassett, and Wyatt Lloyd. 2021. Don't Be a Blockhead: Zoned Namespaces Make Work on Conventional SSDs Obsolete. In *Proceedings of the Workshop on Hot Topics in Operating Systems* (Ann Arbor Michigan, 2021-06). ACM, 144–151. <https://doi.org/10.1145/3458336.3465300>
- [84] The Epoch AI. 2023. Announcing Epoch AI's Updated Parameter, Compute and Data Trends Database. <https://epochai.org/blog/announcing-updated-pcd-database>. Accessed 07/21/2024.
- [85] Hugo Touvron, Louis Martin, Kevin Stone, Peter Albert, Amjad Almahairi, Yasmine Babaei, Nikolay Bashlykov, Soumya Batra, Prajjwal Bhargava, Shrutit Bhosale, Dan Bikel, Lukas Blecher, Cristian Canton Ferrer, Moya Chen, Guillem Cucurull, David Esiobu, Jude Fernandes, Jeremy Fu, Wenyin Fu, Brian Fuller, Cynthia Gao, Vedanuj Goswami, Naman Goyal, Anthony Hartshorn, Saghar Hosseini, Rui Hou, Hakan Inan, Marcin Kardas, Viktor Kerkez, Madian Khabsa, Isabel Kloumann, Artem Korenev, Punit Singh Koura, Marie-Anne Lachaux, Thibaut Lavril, Jenya Lee, Diana Liskovich, Yinghai Lu, Yuning Mao, Xavier Martinet, Todor Mihaylov, Pushkar Mishra, Igor Molybog, Yixin Nie, Andrew Poulton, Jeremy Reizenstein, Rashi Rungta, Kalyan Saladi, Alan Schelten, Ruan Silva, Eric Michael Smith, Ranjan Subramanian, Xiaoqing Ellen Tan, Binh Tang, Ross Taylor, Adina Williams, Jian Xiang Kuan, Puxin Xu, Zheng Yan, Iliyan Zarov, Yuchen Zhang, Angela Fan, Melanie Kambadur, Sharan Narang, Aurelien Rodriguez, Robert Stojnic, Sergey Edunov, and Thomas Scialom. 2023. Llama 2: Open Foundation and Fine-Tuned Chat Models. <https://doi.org/10.48550/arXiv.2307.09288> arXiv:2307.09288 [cs]
- [86] Ashish Vaswani, Noam Shazeer, Niki Parmar, Jakob Uszkoreit, Llion Jones, Aidan N Gomez, Łukasz Kaiser, and Illia Polosukhin. 2017. Attention Is All You Need. In *Advances in Neural Information Processing Systems*, Vol. 30. Curran Associates, Inc.
- [87] Linnan Wang, Jinmian Ye, Yiyang Zhao, Wei Wu, Ang Li, Shuaiwen Leon Song, Zenglin Xu, and Tim Kraska. 2018. SuperNeurons: Dynamic GPU Memory Management for Training Deep Neural Networks. In *Proceedings of the 23rd ACM SIGPLAN Symposium on Principles and Practice of Parallel Programming*. 41–53. <https://doi.org/10.1145/3178487.3178491> arXiv:1801.04380 [cs]
- [88] Jason Wei, Yi Tay, Rishi Bommasani, Colin Raffel, Barret Zoph, Sebastian Borgeaud, Dani Yogatama, Maarten Bosma, Denny Zhou, Donald Metzler, Ed H. Chi, Tatsunori Hashimoto, Oriol Vinyals, Percy Liang, Jeff Dean, and William Fedus. 2022. *Emergent Abilities of Large Language Models*. arXiv:2206.07682 [cs] <http://arxiv.org/abs/2206.07682>
- [89] Wikipedia. 2006. Monkey Patch. https://en.wikipedia.org/w/index.php?title=Monkey_patch&oldid=1216352798
- [90] BigScience Workshop, Teven Le Scao, Angela Fan, Christopher Akiki, Ellie Pavlick, Suzana Ilić, Daniel Hesslow, Roman Castagné, Alexandra Sasha Luccioni, François Yvon, Matthias Gallé, Jonathan Tow, Alexander M. Rush, Stella Biderman, Albert Webson, Pawan Sasanka Ammanamanchi, Thomas Wang, Benoît Sagot, Niklas Muennighoff, Albert Villanova del Moral, Olatunji Ruwase, Rachel Bawden, Stas Bekman, Angelina McMillan-Major, Iz Beltagy, Huu Nguyen, Lucile Saulnier, Samson Tan, Pedro Ortiz Suarez, Victor Sanh, Hugo Laurençon, Yacine Jernite, Julien Launay, Margaret Mitchell, Colin Raffel, Aaron Gokaslan, Adi Simhi, Aitor Soroa, Alham Fikri Aji, Amit Alfassy, Anna Rogers, Ariel Kreisberg Nitzav, Canwen Xu, Chenghao Mou, Chris Emezue, Christopher Klamm, Colin Leong, Daniel van Strien, David Ifeoluwa Adelani, Dragomir Radev, Eduardo González Ponferrada, Efrat Levkovizh, Ethan Kim, Eyal Bar Natan, Francesco De Toni, Gérard Dupont, Germán Kruszewski, Giada Pistilli, Hady Elsahar, Hamza Benyamina, Hieu Tran, Ian Yu, Idris Abdulmumin, Isaac Johnson, Itziar Gonzalez-Dios, Javier de la Rosa, Jenny Chim, Jesse Dodge, Jian Zhu, Jonathan Chang, Jörg Froberg, Joseph Tobing, Joydeep Bhattacharjee, Khalid Almubarak, Kimbo Chen, Kyle Lo, Leandro Von Werra, Leon Weber, Long Phan, Loubna Ben allal, Ludovic Tanguy, Manan Dey, Manuel Romero Muñoz, Maraim Masmoud, Maria Grandury, Mario Šaško, Max Huang, Maximin Coavoux, Mayank Singh, Mike Tian-Jian Jiang, Minh Chien Vu, Mohamad A. Jauhar, Mustafa Ghaleb, Nishant Subramani, Nora Kassner, Nurulaqilla Khamis, Olivier Nguyen, Omar Espejel, Ona de Gibert, Paulo Villegas, Peter Henderson, Pierre Colombo, Priscilla Amuok, Quentin Lhoest, Rhea Harliman, Rishi Bommasani, Roberto Luis López, Rui Ribeiro, Salomey Osei, Sampo Pyysalo, Sebastian Nagel, Shamik Bose, Shamsuddeen Hassan Muhammad, Shanya Sharma, Shayne Longpre, Somaieh Nikpoor, Stanislav Silberberg, Suhas Pai, Sydney Zink, Tiago Timponi Torrent, Timo Schick, Tristan Thrush, Valentin Danchev, Vassilina Nikoulina, Veronika Laippala, Violette Lepercq, Vrinda Prabhu, Zaid Alyafeai, Zeerak Talat, Arun Raja, Benjamin Heinzerling, Chenglei Si, Davut Emre Taşar, Elizabeth Salesky, Sabrina J. Mielke, Wilson Y. Lee, Abheesht Sharma, Andrea Santilli, Antoine Chaffin, Arnaud Stiegler, Debajyoti Datta, Eliza Szczechla, Gunjan Chhablani, Han Wang, Harshit Pandey, Hendrik Strobelt, Jason Alan Fries, Jos Rozen, Leo Gao, Lintang Sutawika, M. Saiful Bari, Maged S. Al-shaibani, Matteo Manica, Nihal Nayak, Ryan Teehan, Samuel Albanie, Sheng Shen, Srulik Ben-David, Stephen H. Bach, Taewoon Kim, Tali Bers, Thibault Fevry, Trishala Neeraj, Urmish Thakker, Vikas Raunak, Xianguo Tang, Zheng-Xin Yong, Zhiqing Sun, Shaked Brody, Yallow Uri, Hadar Tojarieh, Adam Roberts, Hyung Won Chung, Jaesung Tae, Jason Phang, Ofir Press, Conglong Li, Deepak Narayanan, Hatim Bourfoune, Jared Casper, Jeff Rasley, Max Ryabinin, Mayank Mishra, Minjia Zhang, Mohammad Shoeybi, Myrmin Peyrounette, Nicolas Patry, Nouamane Tazi, Omar Sanseviero, Patrick von Platen, Pierre Cornette, Pierre François Lavallée, Rémi Lacroix, Samyam Rajbhandari, Sanchit Gandhi, Shaden Smith, Stéphane Requeena, Suraj Patil, Tim Dettmers, Ahmed Baruwa, Amanpreet Singh, Anastasia Cheveleva, Anne-Laure Ligozat, Arjun Subramonian, Aurélie Névéol, Charles Lovering, Dan Garrette, Deepak Tunuguntla, Ehud Reiter, Ekaterina Taktasheva, Ekaterina Voloshina, Eli Bogdanov, Genta Indra Winata, Hailey Schoelkopf, Jan-Christoph Kalo, Jekaterina Novikova, Jessica Zosa Forde, Jordan Clive, Jungo Kasai, Ken Kawamura, Liam Hazan, Marine Carpuat, Miruna Clinciu, Najoung Kim, Newton Cheng, Oleg Serikov, Omer Antverg, Oskar van der Wal, Rui Zhang, Ruochen

- Zhang, Sebastian Gehrmann, Shachar Mirkin, Shani Pais, Tatiana Shavrina, Thomas Scialom, Tian Yun, Tomasz Limisiewicz, Verena Rieser, Vitaly Protasov, Vladislav Mikhailov, Yada Pruksachatkun, Yonatan Belinkov, Zachary Bamberger, Zdeněk Kasner, Alice Rueda, Amanda Pestana, Amir Feizpour, Ammar Khan, Amy Faranak, Ana Santos, Anthony Hevia, Antigona Unldreaj, Arash Aghagol, Arezoo Abdollahi, Aycha Tammour, Azadeh HajiHosseini, Bahareh Behroozi, Benjamin Ajibade, Bharat Saxena, Carlos Muñoz Ferrandis, Daniel McDuff, Danish Contractor, David Lansky, Davis David, Douwe Kiela, Duong A. Nguyen, Edward Tan, Emi Baylor, Ezinwanne Ozoani, Fatima Mirza, Frankline Ononiwu, Habib Rezanejad, Hessie Jones, Indrani Bhattacharya, Irene Solaiman, Irina Sedenko, Isar Nejadgholi, Jesse Passmore, Josh Seltzer, Julio Bonis Sanz, Livia Dutra, Mairon Samagaio, Maraim Elbadri, Margot Mieskes, Marissa Gerchick, Martha Akinlolu, Michael McKenna, Mike Qiu, Muhammed Ghauri, Mykola Burynek, Nafis Abrar, Nazneen Rajani, Nour Elkott, Nour Fahmy, Olanrewaju Samuel, Ran An, Rasmus Kromann, Ryan Hao, Samira Alizadeh, Sar-mad Shubber, Silas Wang, Sourav Roy, Sylvain Viguier, Thanh Le, Tobi Oyebade, Trieu Le, Yoyo Yang, Zach Nguyen, Abhinav Ramesh Kashyap, Alfredo Palasciano, Alison Callahan, Anima Shukla, Antonio Miranda-Escalada, Ayush Singh, Benjamin Beilharz, Bo Wang, Caio Brito, Chenxi Zhou, Chirag Jain, Chuxin Xu, Clémentine Fourier, Daniel León Perrián, Daniel Molano, Dian Yu, Enrique Manjavacas, Fabio Barth, Florian Fuhrmann, Gabriel Altay, Giyaseddin Bayrak, Gully Burns, Helena U. Vrabec, Imane Bello, Ishani Dash, Jihyun Kang, John Giorgi, Jonas Golde, Jose David Posada, Karthik Rangasai Sivaraman, Lokesh Bulchandani, Lu Liu, Luisa Shinzato, Madeleine Hahn de Bykhovetz, Maiko Takeuchi, Marc Pàmies, Maria A. Castillo, Marianna Nezhurina, Mario Sängler, Matthias Samwald, Michael Cullan, Michael Weinberg, Michiel De Wolf, Mina Mihaljcic, Minna Liu, Moritz Freidank, Myungsun Kang, Natasha Seelam, Nathan Dahlberg, Nicholas Michio Broad, Nikolaus Muellner, Pascale Fung, Patrick Haller, Ramya Chandrasekhar, Renata Eisenberg, Robert Martin, Rodrigo Canalli, Rosaline Su, Ruisi Su, Samuel Cahyawijaya, Samuele Garda, Shlok S. Deshmukh, Shubhanshu Mishra, Sid Kiblawi, Simon Ott, Sincee Sang-aaroonsiri, Srishti Kumar, Stefan Schweter, Sushil Bharati, Tanmay Laud, Théo Gigant, Tomoya Kainuma, Wojciech Kusa, Yanis Labrak, Yash Shailesh Bajaj, Yash Venkatraman, Yifan Xu, Yingxin Xu, Yu Xu, Zhe Tan, Zhongli Xie, Zifan Ye, Mathilde Bras, Younes Belkada, and Thomas Wolf. 2023. BLOOM: A 176B-Parameter Open-Access Multilingual Language Model. arXiv:2211.05100 [cs]
- [91] Yuanzhong Xu, HyoukJoong Lee, Dehao Chen, Blake Hechtman, Yanping Huang, Rahul Joshi, Maxim Krikun, Dmitry Lepikhin, Andy Ly, Marcello Maggioni, Ruoming Pang, Noam Shazeer, Shibo Wang, Tao Wang, Yonghui Wu, and Zhifeng Chen. 2021. GSPMD: General and Scalable Parallelization for ML Computation Graphs. arXiv:2105.04663 [cs]
- [92] Manzil Zaheer, Guru Guruganesh, Avinava Dubey, Joshua Ainslie, Chris Alberti, Santiago Ontanon, Philip Pham, Anirudh Ravula, Qifan Wang, Li Yang, and Amr Ahmed. 2020. Big Bird: Transformers for Longer Sequences. In *Proceedings of the 34th International Conference on Neural Information Processing Systems* (Red Hook, NY, USA, 2020-12-06) (*NIPS '20*). Curran Associates Inc., 17283–17297.
- [93] Ningxin Zheng, Bin Lin, Quanlu Zhang, Lingxiao Ma, Yuqing Yang, Fan Yang, Yang Wang, Mao Yang, and Lidong Zhou. 2022. SparTA: Deep-Learning Model Sparsity via Tensor-with-Sparsity-Attribute. In *Proceedings of the 16th USENIX Symposium on Operating Systems Design and Implementation* (Carlsbad, CA, USA, 2022-07-11).
- [94] Aojun Zhou, Yukun Ma, Junnan Zhu, Jianbo Liu, Zhijie Zhang, Kun Yuan, Wenxiu Sun, and Hongsheng Li. 2021. *Learning N:M Fine-grained Structured Sparse Neural Networks From Scratch*. arXiv:2102.04010 [cs] <http://arxiv.org/abs/2102.04010>